

# Preparation and *In Vitro* Degradation of Novel Bioactive Poly(lactide)/Wollastonite Scaffolds

Liang Xu,<sup>1,2,3</sup> Zuo Chun Xiong,<sup>2,3</sup> Dejuan Yang,<sup>2</sup> Li Fang Zhang,<sup>2,3</sup> Jiang Chang,<sup>4</sup> Cheng Dong Xiong<sup>2</sup>

<sup>1</sup>ChongQing University of Technology, ChongQing 400050, People's Republic of China

<sup>2</sup>Chengdu Institute of Organic Chemistry, Chinese Academy of Sciences, Chengdu 610041, People's Republic of China

<sup>3</sup>Graduate School of the Chinese Academy of Sciences, Beijing 100039, People's Republic of China

<sup>4</sup>ShangHai Institute of Ceramics, Chinese Academy of Sciences, ShangHai 200050, People's Republic of China

Received 16 July 2007; accepted 27 February 2008

DOI 10.1002/app.28475

Published online 12 August 2009 in Wiley InterScience (www.interscience.wiley.com).

**ABSTRACT:** Composite scaffolds for applications in bone engineering from poly(D,L-lactide) (PDLLA) incorporated with different proportional bioactive wollastonite powders were prepared through a salt-leaching method, using  $\text{NH}_4\text{HCO}_3$  as porogen. The pore structures and morphology of the scaffolds were determined by scanning electron microscopy (SEM). The bioactivity of composite materials was evaluated by examining its ability to initiate the formation of hydroxyapatite ( $\text{Ca}_{10}(\text{PO}_4)_6(\text{OH})_2$ )(HAp) on its surface when immersed in simulated body fluids (SBF). The *in vitro* degradation behaviors of these scaffolds were systematically monitored at varying time periods of 1, 2, 4, 6, 8, 11, 14, 17, 20, 24, and 28 weeks postimmersion in SBF at 37°C. FT-IR, XPS, XRD, and SEM measurements

revealed that hydroxyapatite commenced to form on the surface of the scaffolds after 7 days of immersion in SBF. The measurements of weight loss, pH, and molecular weight of the samples indicated that PDLLA/wollastonite composite scaffolds degraded slower than the pure PDLLA scaffolds do. Addition of wollastonite enhanced the mechanical property of the composite scaffolds. The *in vitro* osteoblast culture experiment confirmed the biocompatibility of the scaffold for the growth of osteoblasts. © 2009 Wiley Periodicals, Inc. *J Appl Polym Sci* 114: 3396–3406, 2009

**Key words:** poly(D,L-lactide); wollastonite; scaffold; degradation; biocompatibility

## INTRODUCTION

Cells or bioactive substances such as growth factor that may benefit the ingrowth of the cells are introduced into composite scaffolds to make them biological substitutes for defective tissues and to help them regenerate natural tissues. Poly( $\alpha$ -hydroxyesters) such as poly(lactic acid), poly(glycolic acid), and their copolymers have been widely used to fabricate different kinds of scaffolds in tissue engineering because of their good biodegradability, biocompatibility, and plasticity.<sup>1–3</sup> However, there are a few problems when considering the practical use of these polymers for tissue engineering. One of the limitations of these polymers is the lack of bioactivity so that the new bone tissue cannot bond to the polymer surface tightly when they apply for the bone tissue growth.<sup>4</sup> Another problem is their poor mechanical property.

Hench and Paschall have shown the integral role that silica plays in the bioactivity and osteogenic potential of bioglass in the early 1970s.<sup>5</sup> Their biological investigation has revealed that silicon may play an important role in the early stage of bone calcification

while it is associated with calcium.<sup>6</sup> Since then a great deal of interests have focused on the development of different kinds of biomaterials containing Ca—Si, such as bioactive glasses,<sup>7</sup> apatite/wollastonite (A/W) glass-ceramics,<sup>8</sup> and pseudowollastonite.<sup>9–11</sup>

Wollastonite is a naturally occurring calcium silicate, which has been widely used as filler in polymers to fabricate composites with improved mechanical properties.<sup>12–14</sup> Recent studies have shown that wollastonite was bioactive, and it might be used as bioactive material in tissue repair or tissue-engineering research.<sup>15</sup>

Here, we fabricated novel bioactive and porous composite scaffolds by blending wollastonite powders into PDLLA, so that it integrated the advantages of the both phases while minimizing the limitations of each.

## EXPERIMENTAL

### Materials

Poly(D,L-lactide)(PDLLA,  $\eta = 3.94$  dL/g) was provided by Sichuan Dikang Sci and Tech Pharmaceutical Co. Ltd. (Chengdu, China). Wollastonite powders (2500 meshes,  $L/D$ : 6–10) with particle size of 2–5  $\mu\text{m}$  was purchased from ShangHai Institute of Ceramics Chinese Academy of Sciences (ShangHai,

Correspondence to: C. D. Xiong (xcd@cioc.ac.cn).

China). The components of the wollastonite include SiO<sub>2</sub> (48–52%) and CaO (42–46%).

### Fabrication of PDLLA/wollastonite porous scaffold

Macroporous PDLLA/wollastonite (P/W) scaffold was made by a salt-leaching method. The wollastonite powders were dispersed in 30 mL 1,4-dioxane solvent under stirring, and then the definite quantitative PDLLA was added into this suspension. By maintaining the mixtures for 8 h at 25°C, an elastic gel was produced. The elastic polymer–wollastonite gel was mixed homogeneously with sieved NH<sub>4</sub>HCO<sub>3</sub> salt particles (salt particle size: 150–250 μm; weight ratio of salt/PDLLA and wollastonite: 6/1). The mixture of polymer/wollastonite/salt was cast into a disk-shaped glass mold (10 mm in diameter and 5 mm in thickness), then quenched in liquid nitrogen and freeze-dried. After 72 h, the solid samples with micropore were removed from the freeze-dryer and immersed in distilled water for 48 h to leach the salt out. While doing this, the distilled water was refreshed at every 4-h interval. The samples were then placed in a vacuum-dryer for 72 h at 25°C to remove the remaining solvent. The P/W scaffolds obtained by this method possessed highly interconnected macropores (300–450 μm) and high porosity. In this test, the scaffolds with different proportion [PDLLA/wollastonite = 100/0(P), 90/10(P/W10), 80/20(P/W20), 70/30(P/W30)] were prepared.

### Porosity of P/W porous scaffold

The open porosity was calculated by the liquid displacement method.<sup>16–18</sup> The scaffolds were submerged in a known volume ( $V_1$ ) of ethanol, and a series of brief evacuation repressurization cycles was conducted to force the liquid into the pores of the scaffold. After these cycles, the volume of the liquid together with liquid-impregnated scaffold is  $V_2$ . When the liquid-impregnated scaffold is removed, the remaining liquid volume is  $V_3$  and open porosity is given as

$$\pi = \frac{V_1 - V_3}{V_2 - V_3}$$

### Degradation experiments

The *in vitro* degradation properties were evaluated in simulated body fluid (SBF) as the release medium. Three parallel samples taken from a certain sort of scaffolds were immersed in 20 mL SBF, four different sorts of scaffolds were set as a group, 11 identical sample groups were set to investigate the degradation of different scaffolds of different degradation

durations. To prepare the SBF, dissolved NaCl, NaHCO<sub>3</sub>, KCl, K<sub>2</sub>HPO<sub>4</sub>·3H<sub>2</sub>O, MgCl<sub>2</sub>·6H<sub>2</sub>O, CaCl<sub>2</sub>, and Na<sub>2</sub>SO<sub>4</sub> in ultrapure water and buffered the solution to pH 7.40 at 37.5°C with Tris(hydroxymethyl) aminomethane (final concentration of 50 mM) and aqueous 1M HCl solution.<sup>19</sup> Ion concentrations of the SBF are Na<sup>+</sup> 142.0, K<sup>+</sup> 5.0, Mg<sup>2+</sup> 1.5, Ca<sup>2+</sup> 2.5, Cl<sup>-</sup> 147.8, HCO<sub>3</sub><sup>-</sup> 4.2, HPO<sub>4</sub><sup>2-</sup> 1.0, SO<sub>4</sub><sup>2-</sup> 0.5 mM, approximate the human blood plasma. The scaffolds were then sealed and put into an incubator of constant temperature 37.5°C. The SBF solution was replaced every 3 days with freshly prepared SBF to compensate for the cation decrease over the course of the *in vitro* studies. Scaffolds were removed at predetermined time intervals of 1, 2, 4, 6, 8, 11, 14, 17, 20, 24, and 28 weeks, respectively. These samples were gently rinsed with distilled water before drying for 48 h in an incubator that maintained a temperature of 37°C and controlled relative humidity of 30%. The measurements of weight loss, pH, and molecular weight of the samples were then determined. The pure PDLLA scaffolds served as controls.

### FT-IR

FT-IR spectra analysis for P/W composite scaffold (P/W10) and the deposition on the surface of the composite scaffold (P/W10) were recorded using NICOLET 200SXV FT-IR (USA) spectrometer with a wave number resolution of 2 cm<sup>-1</sup>. The samples were mixed with KBr and made into slices. The wave number was between 4000 cm<sup>-1</sup> and 450 cm<sup>-1</sup>.

### Scanning electron microscopy

The surface of predeposited and deposited the pure PDLLA scaffold and the P/W composite scaffolds were examined using SEM (KYKY-AMRAY 1000B).

### X-ray photoelectron spectroscopy

The component of the deposition is also certified by the X-ray photoelectron spectroscopy diffractometer (XPS, X SAM-800), using an X-ray source (Al Kα, 12 kV × 12mA) with a 45.0 source analyzer angle.

### X-ray diffraction

The X-ray diffraction (XRD) experiments of the predeposited and deposited the P/W composite scaffolds were carried out using a Philips X'Pert Pro XRD that was equipped with a Ni-filtered Cu Kα (λ = 0.1542 nm) radiation source operated at a voltage of 40 kV and a current of 30 mA. Samples were scanned from 15 to 80° (2θ). The step size and time

for each step were  $0.02^\circ$  and 1 s per step, respectively.

### Mechanical properties

The compressive properties of the scaffolds including compressive strength and compressive modulus were measured by the dynamical mechanical analyzer (Testometric AXM 350-10KN). Each circular specimen with 9 mm diameter and 7 mm thickness was dipped in distilled water for 1 h at  $25^\circ\text{C}$  and then compressed at a compress rate of 2 mm/min. The compressive offset yield stress was determined from the stress-strain curve at a 2% strain. The compressive modulus of per sample was obtained by averaging five measurements, and expressed as mean  $\pm$  SD.

### Cell culture

The immortalized rat osteoblastic ROS 17/2.8 cell line (obtained from The West China College of Medicine, Sichuan University) was utilized in this study. These cells were incubated in a humidified atmosphere of 5%  $\text{CO}_2$  at  $37^\circ\text{C}$ . Culture media and supplements were obtained from Invitrogen (Paisley, UK). Osteoblast cells were cultured in Dulbecco's modified Eagle's medium supplemented with 10% fetal calf serum, 100 mg/mL streptomycin, and 100 U/mL penicillin. The culture media was changed every alternate day.

The pure PDLLA scaffold and the P/W composite scaffold (P/W30) were cut into round slices (9 mm in diameter and 1 mm in thickness). And after disinfecting with  $\gamma$ -ray, these samples were placed into 24-well plate, then  $1 \times 10^4$  cells in 1 mL medium were added to the well and osteoblasts allowed to settle onto the composite scaffold and pure PDLLA scaffold discs. All experiments were cultured at  $37^\circ\text{C}$  in a humidified atmosphere with 5%  $\text{CO}_2$ . Medium was changed every 3 days. Time points of 1, 3, and 6 days were studied from the day of cell seeding.

### MTT assay

The 3-[4,5-dimethylthiazol-2-yl]-2,5-diphenyltetrazolium bromide (MTT) assay measures mitochondrial succinate dehydrogenase activity to assess cell number. Osteoblasts were seeded onto the pure PDLLA scaffold and composite scaffold (P/W30) ( $1 \times 10^4$  cells/well) in a 24-well plate in triplicate and incubated at  $37^\circ\text{C}$ . The culture medium was replaced every 3 days. After days 1, 3, and 6, 200  $\mu\text{L}$  of MTT (5 mg/mL, Sigma) was added to each well. Cells were then cultured at  $37^\circ\text{C}$  in a humidified atmosphere with 5%  $\text{CO}_2$  for 4 h. Medium was then aspirated off, the samples washed with PBS, and 1 mL

of DMSO (dimethylsulfoxide) were put into each well, then the plate was left on a shaking platform for 10 min to solubilize the tetrazolium, 200  $\mu\text{L}$  of the solution was collected then and pipetted into a 96-well plate and the absorbance was determined at 570 nm according to microplate reader (BIO-RAD, model 550).

### Fluorescent staining and observation

After each time point, the discs of pure PDLLA scaffold and composite scaffold (P/W30) were stained with 0.01% AO (acridine orange) for 5 min, then examined in a fluorescence microscope (OLYMPUS B  $\times 60$ ) after washed with PBS. According to fluorescence observation, living cells would be clearly found on the surface of the composite with cell nucleus in bright green and cytoplasm in orange after blue light excitation, and dead cells would be stained in red.

## RESULTS AND DISCUSSION

### Characterization of P/W composite scaffolds

#### Microstructure analysis by SEM

SEM measurements for the surface morphology of the pure PDLLA scaffold immersed in SBF at the time of 0, 3, and 7 days (P, P-3, P-7) with the magnification of 200 are shown in Figure 1. The pure PDLLA scaffold exhibited macroporous structure with interconnected open pores, and pore size varied from 150 to 250  $\mu\text{m}$ . It is apparent that no deposition was formed as a result of contact of the pure PDLLA scaffold with SBF, and the pore size has not changed obviously with the increase of the time.

Figure 2 shows the morphology ( $\times 200$ ) of the surface of the composite scaffolds with different proportional wollastonite, viz. PW/10 and PW/30 unimmersed in SBF. Compared with the pure PDLLA scaffolds (in Fig. 1), the macroporous structure of the composites was still maintained. And some wollastonite particles dispersed on the surface of pore walls of the composite scaffolds. It could be seen that wollastonite particles were uniformly distributed throughout the PDLLA matrix. When the wollastonite content increased, more particles were apparent on the pore surface and some particles aggregated although the macroporous structure was still maintained. The result indicated the PDLLA and the wollastonite particles were excellently consistent.

The morphology ( $\times 200$ ) of the surface of the composite scaffolds with different wollastonite content immersed in SBF 3 and 7 days measured by SEM is shown in Figure 3. After soaking, it was obvious that the morphology of the scaffold surfaces was



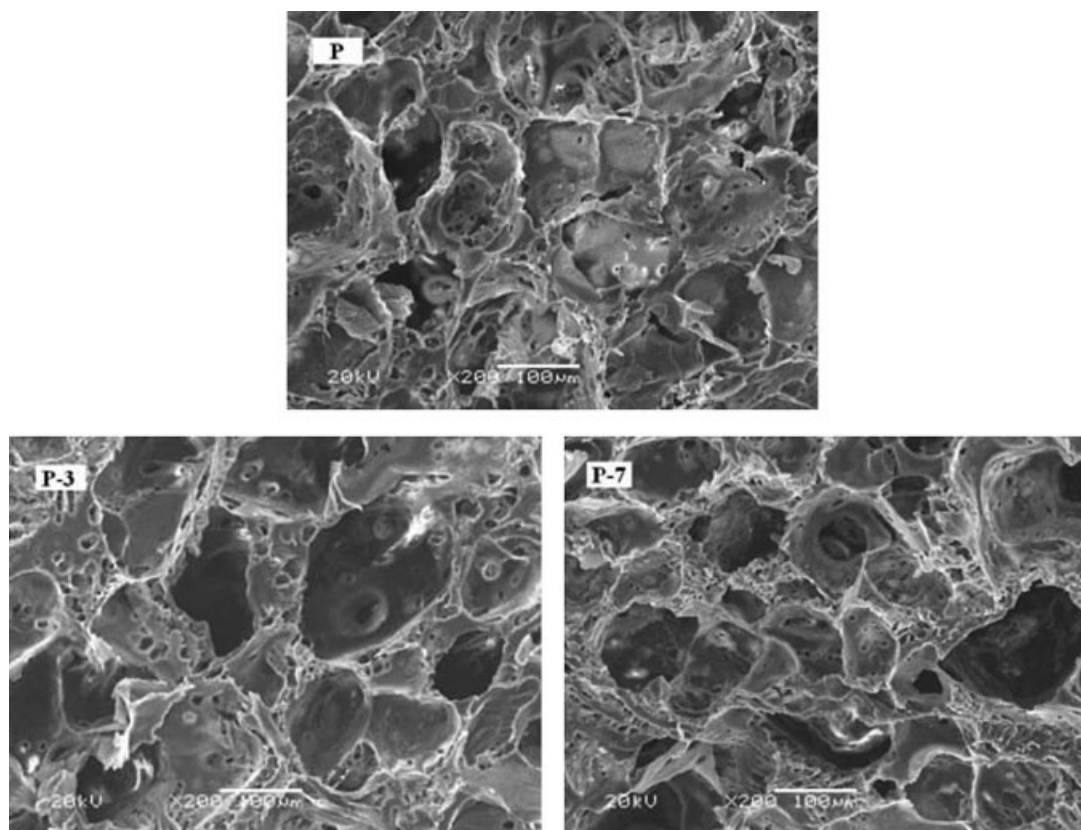


**Figure 1** SEM micrographs of the surface of the pure PDLLA scaffold immersed in SBF 0 day (P), 3 days (P-3), 7 days (P-7).

changed though the pores were still visible. After immersing in SBF for several days, there were some spherical depositions appearing on the surface of the pores, especially 7 days. In addition, when increased wollastonite content of the composite scaffold, spherical depositions on the sample's surface increased. The P/W10-7' is the micrograph of the surface of the P/W10 composite scaffolds after immersion in SBF 7 days with the higher magnification ( $\times 500$ ), which showed that many obvious spherical depositions adhered on the surface of the scaffold's pore wall.

#### Microstructure analysis by FT-IR, XPS, and XRD

For the composite scaffolds, the spherical deposition formed on the surface was investigated using FT-IR, XPS, and XRD, as shown in Figures 4–6.

Figure 4 shows FT-IR spectra of (a) the P/W composite scaffolds with 10 wt % wollastonite and the surface deposition of the composition immersed in SBF (b) 7 days. FT-IR confirmed that deposition formation took place on the scaffold surface after immersion in SBF. Compared with the spectrum of P/W composition (a), the deposition of the composi-

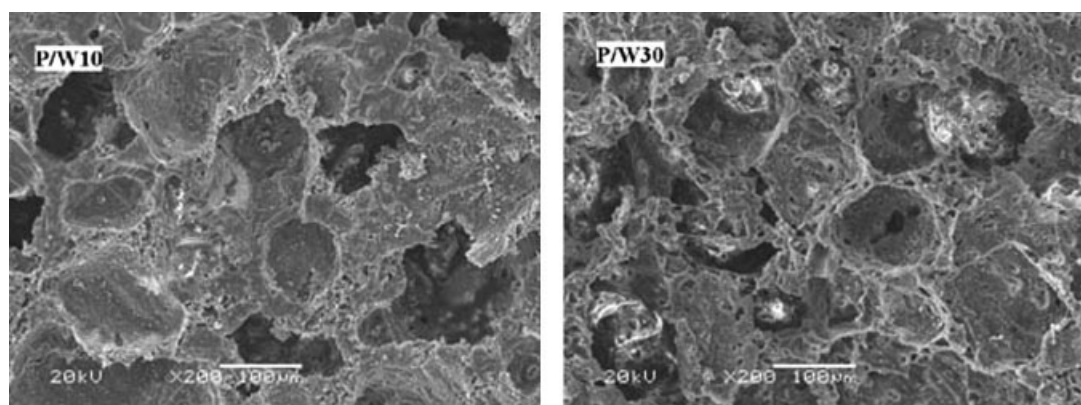


**Figure 2** SEM morphology of the surface of the composite scaffolds with different proportional wollastonite, viz. 10% (P/W10) and 30% (P/W30).

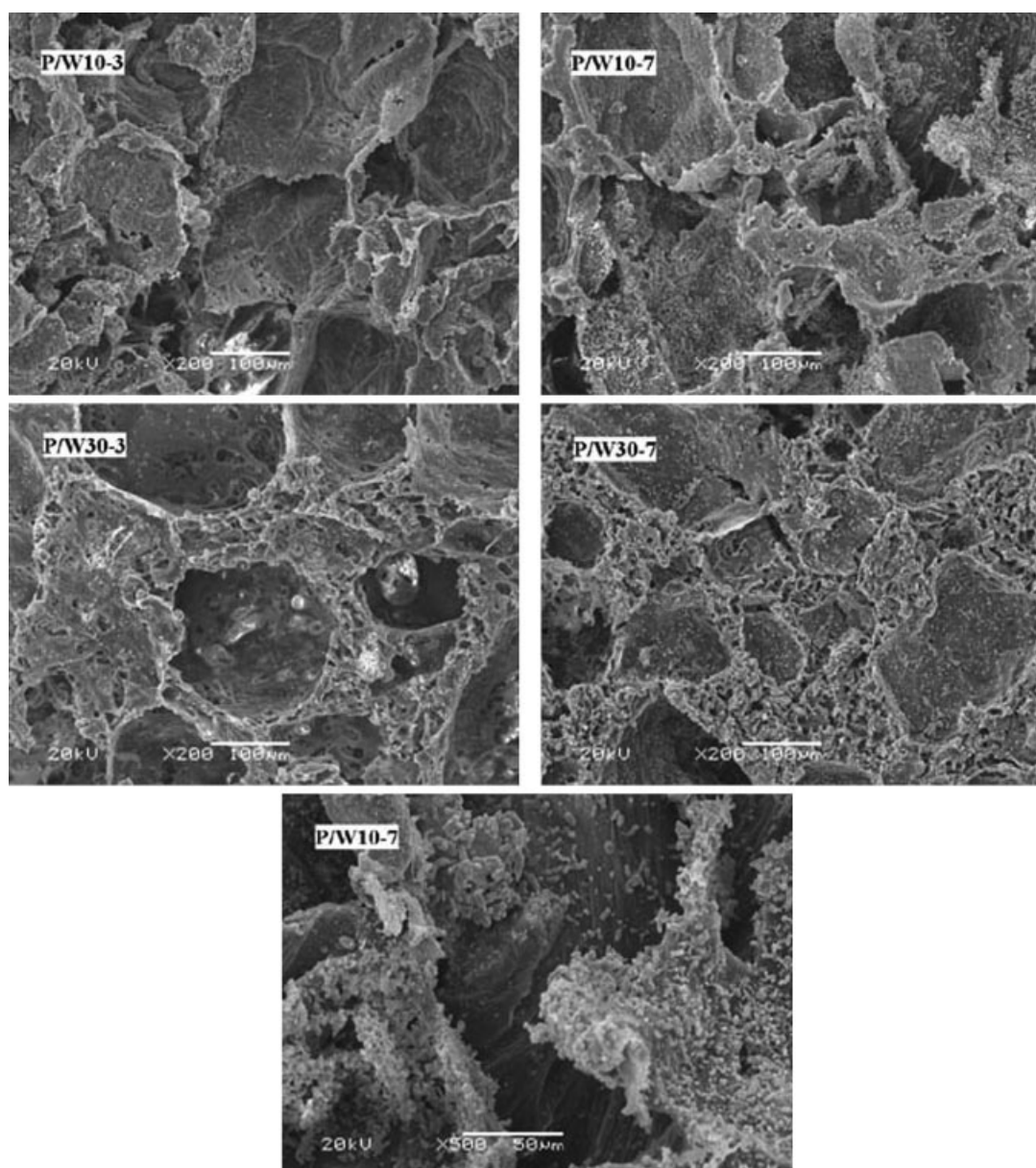


**Figure 3** SEM morphology ( $\times 200$ ) of the surface of the composite scaffolds with different proportional wollastonite immersed in SBF for different days. 10% wollastonite, 3 days (P/W10-3) 10% wollastonite, 7 days (P/W10-7); P/W10-7 ( $\times 500$ ); 30% wollastonite, 3 days (P/W30-3) 30% wollastonite, 7 days (P/W30-7).

tion (b) displayed new absorption bands at wave numbers 563.9, 601.6, and 1039.6  $\text{cm}^{-1}$ . These absorption bands are associated with the characteristics of  $\text{PO}_4^{3-}$ . The absorption at 3449.9  $\text{cm}^{-1}$  was attributed to the O—H of the deposition, closing to the O—H peak of remained  $\text{H}_2\text{O}$ , which can be detected at 3460.8  $\text{cm}^{-1}$  in the (a) curve. The O—H absorption of the deposition covered O—H absorption of  $\text{H}_2\text{O}$  and broadened and strengthened the whole O—H peak. In the spectrum of (a), the absorptions of carboxylic carbonyl band at 1757.7  $\text{cm}^{-1}$ , and the absorption of saturated C—H band at 2995, 2944.8, and 2955.0  $\text{cm}^{-1}$  were the characteristics of PDLLA. The absorption bands at wave number of 455.8 and

471.5  $\text{cm}^{-1}$  are associated with the characteristics of  $\text{SiO}_4^{2-}$ . The absorption bands associated with the characteristics of PDLLA and  $\text{SiO}_4^{2-}$  fade away. It is reasonably to consider from these results that the surface of the specimen was covered with a layer of deposition which might consist of  $\text{Ca}_{10}(\text{PO}_4)_6(\text{OH})_2$ , i.e., HAp.

Figure 5 shows XPS spectra of the crystals formed on the surface of the composite scaffolds with 10 wt % wollastonite after soaking in SBF for 7 days. In Figure 5(a) one peak 132.394 eV ascribed to P of  $\text{PO}_4^{3-}$  was observed. In Figure 5(b) two peaks 347.375 and 350.978 eV ascribed to  $\text{Ca}^{2+}$  were observed. The results certify that the surface deposi-

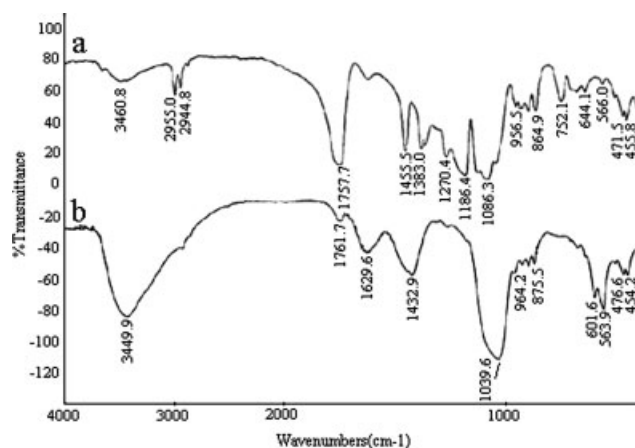


**Figure 4** FT-IR spectra of (a) the composite scaffolds with 10 wt % wollastonite and (b) the deposition on the surface of the composite scaffold with 10 wt % wollastonite immersed in SBF 7 days.

tion comprises both  $\text{Ca}^{2+}$  and  $\text{PO}_4^{3-}$ . From the calculation through the area of the XPS spectra we got the atom ratio between Ca and P, that was 1.68, close to the Ca/P ratio for the HAP (1.67). There was no evidence that HAP crystals were deposited on the surface of the pure PDLLA after soaking in SBF for 7 days. It is obvious from the results described earlier that P/W composite scaffolds is bioactive and could induce deposition of a HAP layer on the surface after exposed in SBF for 7 days.

Figure 6 illustrates XRD graphs of the composite scaffolds with 10 wt % wollastonite before and after immersion in SBF. Compared to the XRD patterns of the composite scaffold unimmersed in SBF, the apatite diffraction peaks at about  $25.6^\circ$ ,  $28.9^\circ$ ,  $31.8^\circ$ ,  $32.9^\circ$ ,  $34^\circ$ ,  $39.8^\circ$ ,  $49.6^\circ$ ,  $53.2^\circ$ ,  $64^\circ$   $2\theta$  were observed in the XRD pattern of the composite scaffold with 10 wt % wollastonite after soaking for 7 days.

Upon degradation, the formation of a calcium-rich surface layer was nucleated beginning with an initial

phase of tricalcium phosphate, followed by precipitation of octacalcium phosphate, which finally served as a template for hydroxyapatite growth. Proverbially, apatite that is analogous to inorganic bone. We hypothesize that the apatite nucleation observed was via the functional groups of the composite scaffold. The scaffold would release positive charged ions, most likely  $\text{Ca}^{2+}$  from wollastonite, into SBF via an exchange with the  $\text{H}_3\text{O}^+$  ions in the fluid to form hydroxyl groups on its surface. These hydroxyl groups would then combine with positive charged ions in the fluid to form an amorphous precipitate on the scaffolds' surface. After a long soaking period, this precipitate combines with phosphate ions in the fluid to form an amorphous calcium phosphate with a low Ca/P ratio and this phase later transforms into bone-like apatite crystal.

### Degradation experiments

The *in vitro* degradation behaviors of these scaffolds which were disinfected by  $\gamma$ -ray were systematically monitored at varying time periods in SBF at  $37^\circ\text{C}$ . It is expected in tissue engineering that the degradation rate of porous polymer scaffolds should be slower than the bone formation rate since the mechanical properties of the scaffolds must be sufficient to support the bone regeneration process.<sup>20</sup>

### Weight loss

The weight loss of the pure PDLLA and P/W composite scaffolds immersed in SBFs is shown in Figure 7.

It is apparent that all the scaffolds showed the gradual increasing trend of weight loss; however, the pure PDLLA scaffold experiences a higher weight loss than the composite scaffolds. The composite scaffolds all displayed a small weight

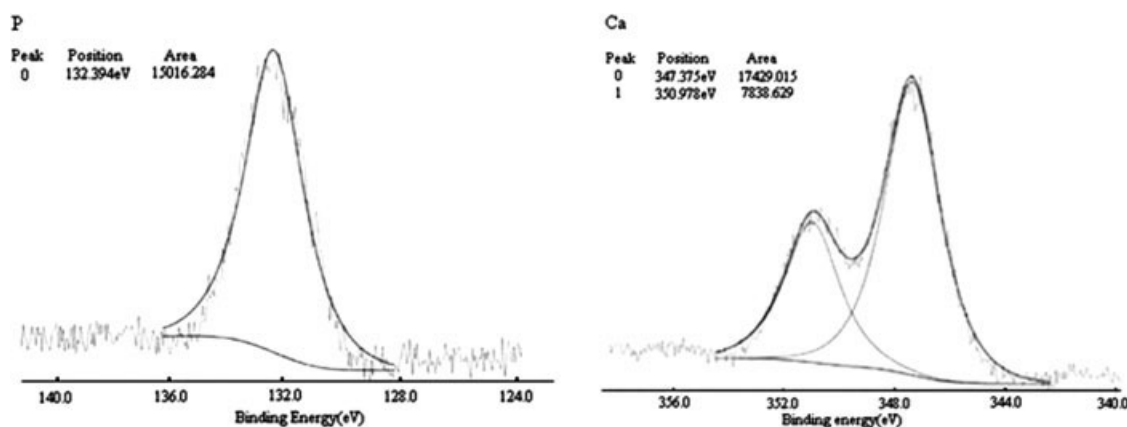


**Figure 5** XPS spectra of the surface deposition of the composite scaffolds with 10 wt % wollastonite immersed in SBF 7 days.



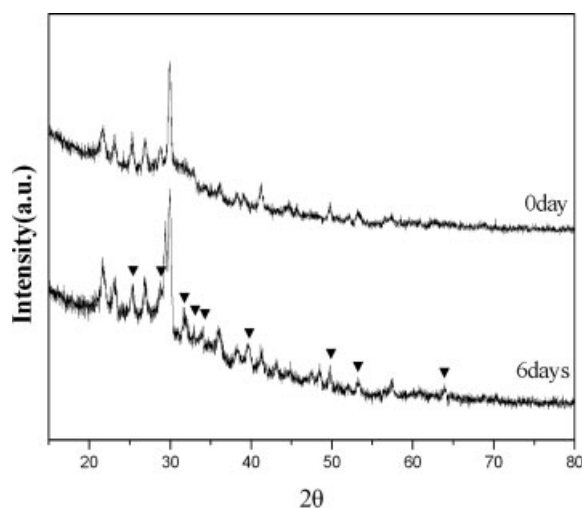


**Figure 6** XRD graphs of the composite scaffolds with 10 wt % wollastonite before and after immersion in SBF 7 days.

increase (<0.1%) at the first 4 weeks. At this early stage of degradation, the deposition occurs on the surface of the scaffold while the weight loss of the scaffolds was neglectable, that led to a slight increase of scaffold weight. During the following degradation, from 6 to 14 weeks all the scaffolds began to lose their weight slowly (<2%). At this stage the rate of chain scission slowed, the hydrolytic process began to produce short chain oligomers and weight loss was observed. PDLLA pure scaffold exhibits a faster increase in weight loss with increasing immersion time, since the acidic produce of the PDLLA scaffolds decreased the PH of the SBF and accelerated the degradation of the scaffold.

From Figure 7, we can find the addition of wollastonite slowed the degradation of PDLLA polymer. When the scaffolds were immersed in solution, the wollastonite particles interacted with the surrounding medium and released alkaline substance to counteract the acidic produce of the hydrolyzation of PDLLA, thus making the mass loss of the composite scaffolds decline slower than that of the pure PDLLA scaffolds does. Since there is a physical bond formed between wollastonite and polylactide, the wollastonite particles tended to fall off from the composite scaffolds and the weight of the composite scaffolds declined sharply after period of time in solution. The falling of wollastonite also created voids within the polymer matrix, which led the surface of the scaffold easily being attacked by hydrolysis.

#### pH measurements

PH measurements for the SBF-soaked samples showed in Figure 8. The pH of the degradation medium was measured with a pH meter (2D-2, Shanghai 2nd Analytical Instruments Factory, China). The pH

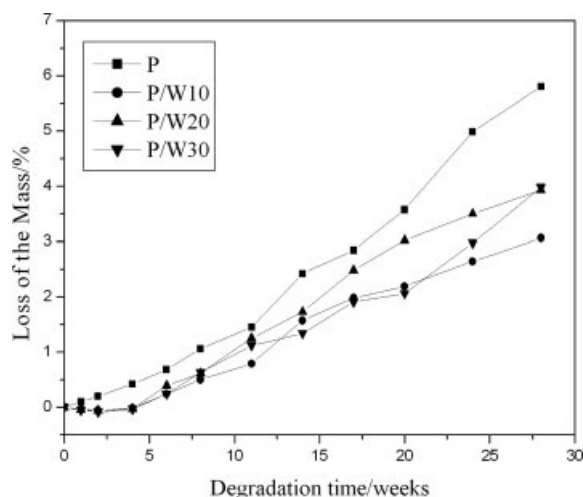


**Figure 7** Weight loss of the pure PDLLA and wollastonite/PDLLA composite scaffolds as a function of degradation time.

of the degradation medium remained a few change during the first 8 weeks, after that it started to decrease quickly till week 20. In the further observation after 20 weeks the PH reached plateau. In Figure 8, the PH of the pure PDLLA scaffold experiences a faster decrease than that of the composite scaffolds with increasing immersion time, since the acidic produce of the PDLLA decreased the PH of the SBF but wollastonite particles could release alkaline substance to counteract such acidic produce from PDLLA to lead a slower decrease of PH compared to that of PDLLA scaffold at the same time interval.

#### Molecular weight

The scaffold specimens after degradation *in vitro* were freeze-dried for 72 h at first and then the scaf-

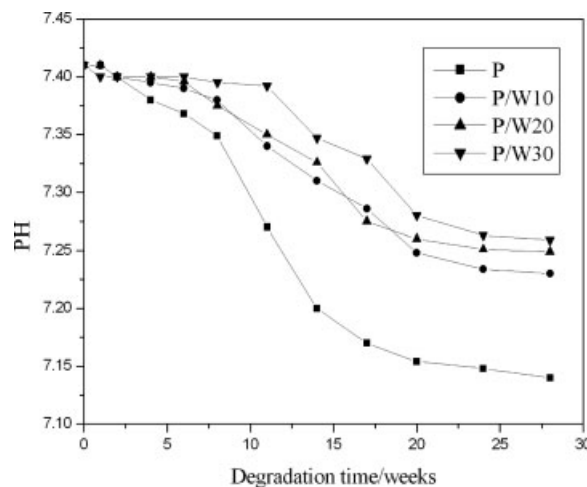


**Figure 8** The pH of the simulated body fluids (SBF) as a function of degradation time.

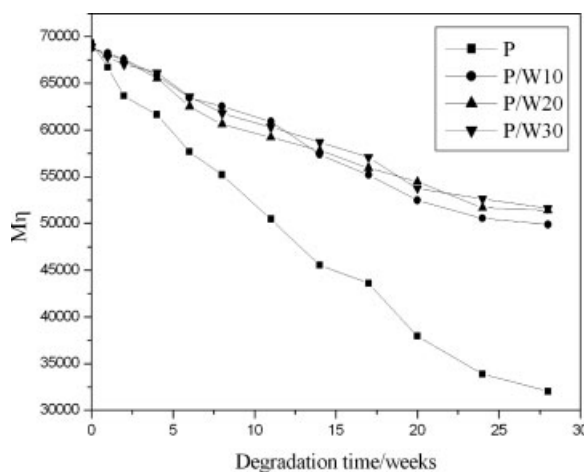


**Figure 9** The viscometric average molecular weight ( $M_n$ ) of the polymeric components in scaffolds as a function of degradation time.

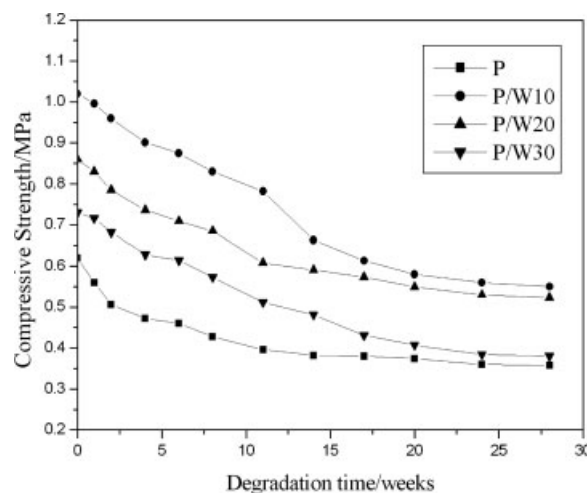
folds were weighed and extracted by chloroform to dissolve all the polymeric components. The polymeric components in the solution were then precipitated from ethanol and dried under vacuum at room temperature for 24 h. Finally, inherent viscosity ( $\eta_{inh}$ ) of the precipitate was measured with an Ubbelohde viscometer thermostated at  $25.0^\circ\text{C} \pm 0.05^\circ\text{C}$  at a concentration of 0.05 g/mL with chloroform as solvent. The viscometric average molecular weight ( $M_n$ ) of the precipitate was calculated by employing the Mark–Houwink constants  $K = 2.21 \times 10^{-4}$  dL/g and  $\alpha = 0.77$ .<sup>21</sup>

Figure 9 shows the changes of the  $M_n$  of the polymeric components in scaffolds as a function of degradation time. Since the scaffolds were disinfected by  $\gamma$ -ray, the initial  $[\eta]_{inh}$  of the samples declined to 1.17 dL/g and the  $M_n$  declined to  $6.87 \times 10^4$ . The  $M_n$  of the three composite scaffolds gave a similar declining trend and lost their values of  $\sim 1.64$ – $1.82 \times 10^4$  after 28 weeks degradation. However, the  $M_n$  of PDLLA scaffold decreased quickly, much faster than the composite scaffolds.

Besides the reasons mentioned earlier, there is another reason for the slowed degradation of P/W scaffolds. Table I showed the porosity of the P/W scaffolds with different proportions. The average porosity of the pure PDLLA scaffold is 86.1%. And with the increase of wollastonite mass in the composite the average porosity of the composite scaffold

**TABLE I**  
The Porosity of PDLLA/Wollastonite Scaffolds with Different Proportions [PDLLA/Wollastonite = 100/0 (P), 90/10 (P/W10), 80/20 (P/W20), 70/30 (P/W30)]

Scaffold	P	P/W10	P/W20	P/W30
Porosity (%)	$86.1 \pm 3.4$	$84.7 \pm 2.9$	$83.5 \pm 3.1$	$82.4 \pm 2.6$



**Figure 10** Plot of the compressive strength of the pure PDLLA scaffolds and the wollastonite/PDLLA composite scaffolds as a function of degradation time.

folds went downwards. The lesser porosity decreased the interaction between the scaffold and the surrounding medium, so the hydrolyzation of PDLLA was slowed.

### Mechanical properties

Since during application of a scaffold in tissue engineering the scaffold will undergo various stresses, to keep scaffold with a certain mechanical strength is necessary. Compared to the bioceramic scaffold, the PDLLA scaffold possesses relatively low mechanical properties. Therefore bioceramics were generally incorporated with the PDLLA scaffold to improve its mechanical properties.<sup>22</sup> Figures 10 and 11 represented the mechanical properties of the scaffolds.

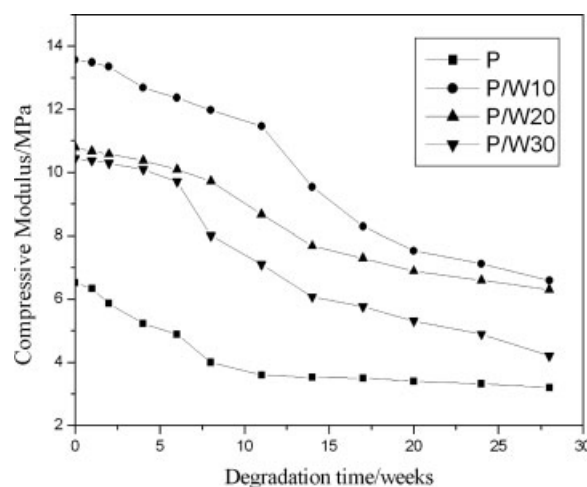


**Figure 11** Plot of the compressive modulus of the pure PDLLA scaffolds and the wollastonite/PDLLA composite scaffolds as a function of degradation time.



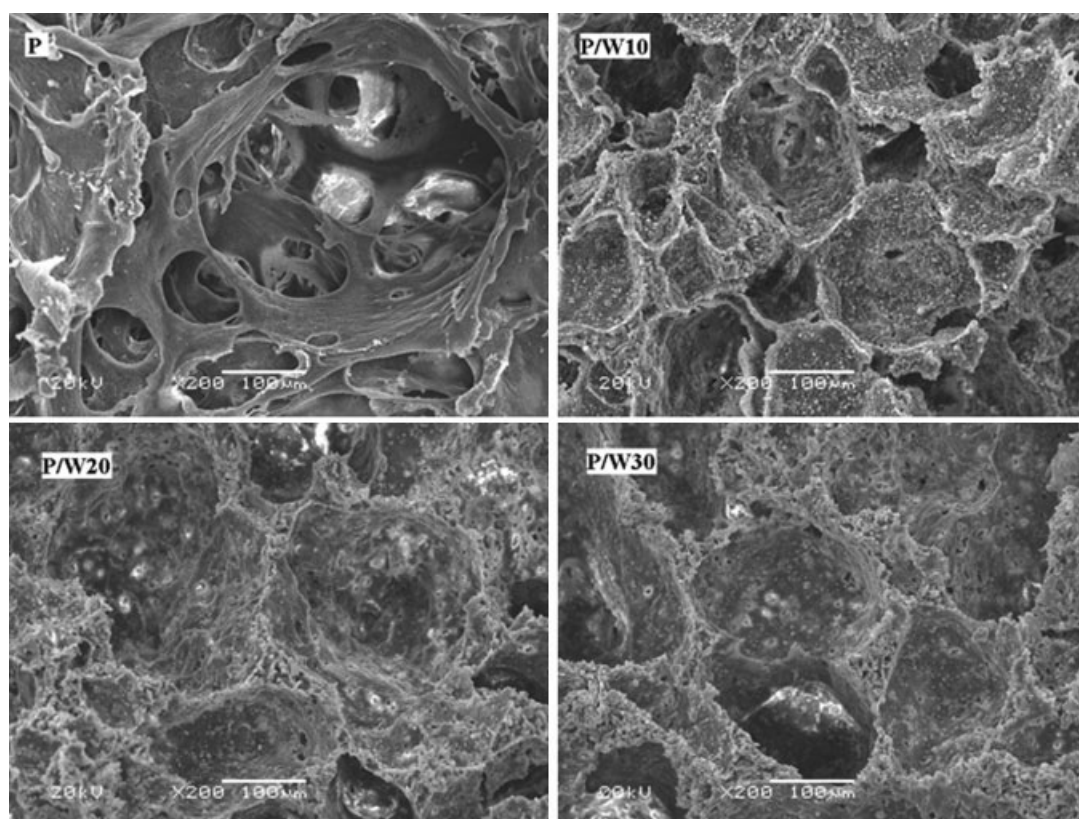


**Figure 12** SEM morphology of the surface of the pure PDLLA scaffold (P) and the composite scaffolds with different proportional wollastonite immersed in SBF for 8 weeks. 10% wollastonite (P/W10); 20% wollastonite (P/W20); 30% wollastonite (P/W30).

Figure 10 shows the plot of compressive strength with immersion time for the pure PDLLA and P/W scaffold specimens during degradation. This figure reveals that the compressive strength of the pure PDLLA and P/W scaffold specimens show similar decrease trend with increasing time of degradation, and they gradually reaches a constant value after degradation of about 11 weeks, except P/W30 which displayed a gradual decrease till 28 weeks. Generally, the compressive strength values of the pure PDLLA scaffold during degradation are lower than those of the P/W composite scaffold, and  $P/W10 > P/W20 > P/W30$ . The initial compressive strength of the scaffold made of 10, 20 and 30% wollastonite reached 1.02, 0.86, and 0.73 MPa which were 1.65, 1.39, and 1.18 times of the pure PDLLA scaffold (0.62 MPa), respectively.

From Figure 11, it could be seen that the compressive modulus of the scaffolds decreased with increasing time of degradation. The compressive modulus values of the pure PDLLA scaffold during degradation are lower than those of the PDLLA/wollastonite composite scaffolds, and  $P/W10 > P/W20 > P/W30$ . For the scaffold made of 10, 20, and 30% wollastonite, the initial compressive modulus of the scaffold were greatly enhanced to about 13.56,

10.8, 10.4, and 4.5 MPa which were 2.08, 1.66, and 1.6 times of the pure PDLLA scaffold, respectively.

The mechanical properties of the pure PDLLA and P/W scaffold all declined with the degradation of PDLLA. In Figures 10 and 11, it could be seen that the compressive strength and compressive modulus of the scaffolds displayed a slow decrease and remained upper values in the initial several weeks and then reduced with further degradation. Subsequently, the compressive modulus of the pure PDLLA scaffold reached a constant value. However, the compressive modulus of the composite scaffolds made of 10, 20, and 30% wollastonite particles displayed a sharp decline at weeks 11, 8, and 6, respectively. That is because the wollastonite revealed and fell off from the PDLLA matrix with the hydrolyzation of the PDLLA, the wollastonite can't be connected steadily with the PDLLA matrix then the mechanical properties of the scaffold declined. And with the increase of the wollastonite particles, the particles were easier to fall off and the compressive modulus displayed an earlier sharp decline.

The reason of the enhancement on mechanical property of the composite scaffolds was considered as the addition of wollastonite particles, which help to form the thicker wall of the scaffold. Comparing

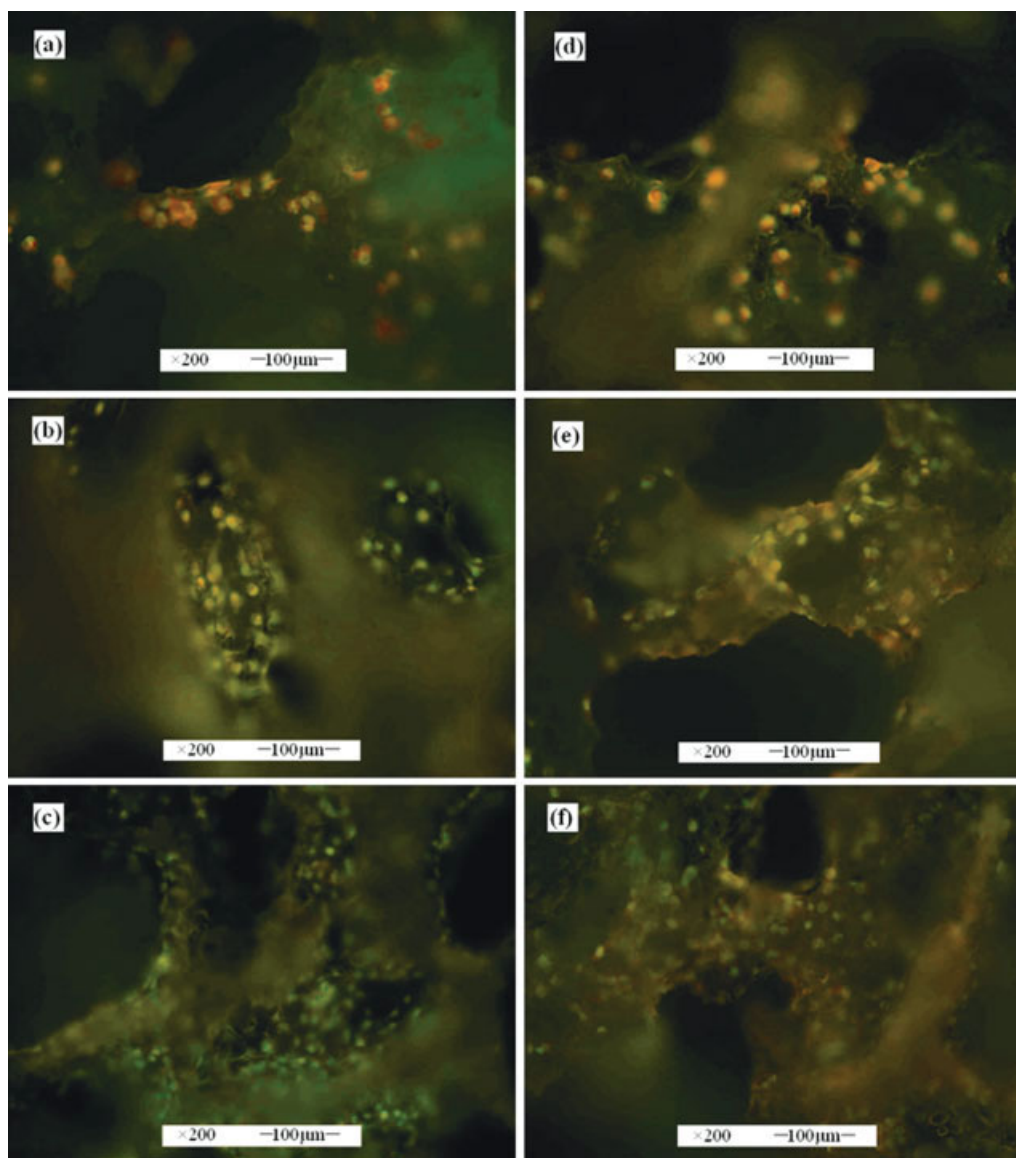


**Figure 13** Fluorescent micrographs of the osteoblasts cultured on the PDLLA scaffolds 1 (a), 3 (b), 6 (c) days and the composition scaffolds with the wollastonite content of 30 wt % 1 (d), 3 (e), 6 (f) days. [Color figure can be viewed in the online issue, which is available at [www.interscience.wiley.com](http://www.interscience.wiley.com).]

sample P (Fig. 1) with samples P/W10, P/W20, P/W30 (Fig. 2), we can see that the wollastonite particles in the walls and the crossings of the pores can support the pore framework better and enhance mechanical properties of the scaffold. Figure 12 showed the surface morphology of the composite scaffolds with different wollastonite contents after an immersion in SBF for 8 weeks. Compared with the pure PDLLA scaffold, the composite scaffolds had preferable scaffold structures. Moreover, the addition of wollastonite particles decreased the porosity of the scaffold (Table I). As a result, the scaffold with a thicker wall that contained wollastonite possessed of higher strength and modulus.

#### Analysis of cytotoxicity and proliferation of the ROS17/2.8 cells

Osteoblasts were cocultured with samples for 1, 3, and 6 days and then assayed for cell viability and proliferation. The Fluorescent micrograph (Fig. 13) of the osteoblasts shows that the osteoblasts seeded onto the two groups of scaffolds all attached to the pore surface and continued to proliferate along the pore walls over time. This result indicated that these two groups of scaffolds all have good biocompatibility for the growth of osteoblasts. A MTT assay was also performed at days 1, 3, and 6 to determine cell growth on the scaffold (Fig. 14). After treatment of the cell-scaffold constructs with the MTT solution,

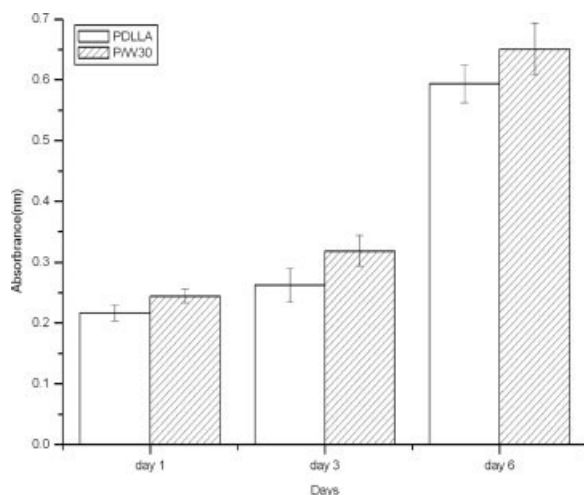


**Figure 14** Cell proliferation assay (MTT). Cells seeded at a density of  $1 \times 10^4$  cell/well for 1, 3, and 6 days. Mean  $\pm$  SD of triplicate independent samples.

dark blue crystals of formazan were seen, indicating the presence of metabolically active cell. The MTT absorption was measured at 570 nm with a background subtraction at 630 nm. A higher absorbance indicates there are either more cells or that they are metabolizing.<sup>23</sup> Figure 14 indicated that there are significant ( $P < 0.05$ ) increases in cell numbers on both the pure PDLLA scaffold and the composite scaffold (P/W30) over time. The result also proved that the two groups of scaffolds all facilitate the growth and proliferation of the osteoblast. However more proliferations in cell numbers were observed on composite scaffold (P/W30) compared to those on PDLLA scaffold.

## CONCLUSIONS

P/W composite scaffolds were prepared by a salt-leaching method. They were degraded slower than the pure PDLLA scaffold by a hydrolytic mechanism when immersed in SBFs. Upon degradation, the P/W scaffolds were bioactive as being confirmed by the formation of the HAp layer on the surface of the composites after immersion in SBF for 7 days. Mechanical properties of the pure PDLLA were

improved after incorporation of wollastonite powders. The *in vitro* cell culture experiment proved that the P/W composite scaffold had good biocompatibility for the growth of the osteoblast. These improved properties, together with the bioactivity, make these scaffolds potential candidates for tissue repair and tissue engineering applications.

## References

- Lu, H. H.; El-Amin, S. F.; Scott, K. D.; Laurencin, C. T. *J Biomed Mater Res* 2003, 64, 465.
- Ishaug-Riley, S. L.; Crane-Kruger, G. M.; Yaszemski, M. J.; Mikos, A. G. *Biomaterials* 1998, 19, 1405.
- Lo, H.; Kadiyala, S.; Guggino, S. E.; Leong, K. W. *J Biomed Mater Res* 1996, 30, 475.
- Schliephake, H.; Neukam, F. W.; Huttmacher, D.; Becker, J. *J Oral Maxillofac Surg* 1994, 52, 57.
- Hench, L. L.; Paschall, H. A. *J Biomed Mater Res* 1973, 7, 25.
- Carlisle, E. M. *Science* 1970, 167, 279.
- Andersson, H. H.; Karlsson, K. H. *J Non-Cryst Solids* 1991, 129, 145.
- Kokubo, T. In *An Introduction to Bioceramics*; Hench, L. L., Wilson, J., Ed.; World Scientific: USA, 1993; p 75.
- De Aza, P. N.; Guitian, F.; De Aza, S. *Scr Metall Mater* 1994, 31, 1001.
- Liu, X. Y.; Ding, C. X.; Wang, Z. Y. *Biomaterials* 2001, 22, 2007.
- De Aza, P. N.; Luklinska, Z. B.; Anseau, M. R.; Guitian, F.; De Aza, S. *J Dent* 1999, 27, 107.
- Tong, J.; Ma, Y.; Jiang, M. *Wear* 2003, 255, 734.
- Low, N. M. P.; Beaudoin, J. *J Cement Concrete Res* 1994, 24, 650.
- Low, N. M. P.; Beaudoin, J. *J Cement Concrete Res* 1994, 24, 874.
- Siriphannon, P.; Kameshima, Y.; Yasumori, A.; Okada, K.; Hayashi, S. *J Eur Ceram Soc* 2002, 22, 511.
- Nazarov, R.; Jin, H. J.; Kaplan, D. L. *Biomacromolecules* 2004, 5, 718.
- Zhang, R.; Ma, P. X. *J Biomed Mater Res* 1999, 44, 446.
- Zhao, F.; Yin, Y.; Lu, W. W.; Leong, J. C.; Zhang, W.; Zhang, J.; Zhang, M.; Yao, K. *Biomaterials* 2002, 23, 3227.
- Kokubo, T.; Kushitani, H.; Sakka, S.; Kitsugi, T.; Yamamuro, T. *J Biomed Mater Res* 1990, 24, 723.
- Hedberg, E. L.; Shih, C. K.; Lemoine, J. J.; Timmer, M. D.; Liebschner, M. A. K.; Jansen, J. A.; Mikos, A. G. *Biomaterials* 2005, 26, 3215.
- Vandijk, J.; Smit, J. *J Polym Sci Polym Chem Ed* 1983, 21, 197.
- Zhang, L. F.; Sun, R.; Xu, L.; Du, J.; Xiong, Z. C.; Chen, H. C.; Xiong, C. D. *Mater Sci Eng C* 2008, 28, 141.
- Molly, M. S.; Hala, F. Q.; Robert, L.; Shastri, V. P. *Biomaterials* 2004, 25, 887.